

## **RIGID-FLEXIBLE COUPLING DYNAMIC ANALYSIS AND TOPOLOGICAL OPTIMIZATION DESIGN OF ROBOT END-EFFECTOR**

Junbin LOU<sup>1,2</sup>, Yaping GONG<sup>3\*</sup>

*The quality stability, high efficiency and rapidity of molding and shaping of pulp products are largely controlled by the structural dynamic characteristics and optimization of the end-effector of the industrial robot. According to the molding process, the rigid-flexible coupling dynamics simulation model of the molding industrial robot and its end-effector was established by using ADAMS dynamics software, and the changing rules of the motion characteristic parameters such as load, speed and acceleration of the end-effector during different processes were analyzed. Based on the goal of lightweight design, the structural optimization design of the end-effector was carried out by topological optimization method, and the structural performance before and after optimization was compared and checked by ANSYS Parametric Design Language (APDL) and Workbench platform. The results show that the equivalent stress of the flexible end-effector reaches the maximum of 150.40 MPa in different process stages, which meets the application requirements of pulp molding. After the optimization, the structural weight of the actuator decreased by 42.16%, the maximum deformation increased by 11.2% and the maximum equivalent stress increased by 19.82%, which realized the lightweight of the structure and basically ensured the mechanical characteristics of the device to meet the application requirements.*

**Keywords:** Pulp molding; Rigid-flexible coupling; Finite element analysis; Topological optimization; End-effector

### **1. Introduction**

Pulp molded products are made of fiber as the main processing raw material, dehydrated by custom-made mold, and then dried, and then dried and shaped. The product has the advantages of cheap and easily available raw materials, pollution-free in the production process, good anti-shock cushioning, ventilation and anti-static performance of products, recyclability and easy

---

<sup>1</sup> Senior Engineer, School of Marine Engineering Equipment, Zhejiang Ocean University, China, e-mail:loujunbin1224@163.com

<sup>2</sup> Senior Engineer, College of Information Science and Engineering, Jiaxing University, China, e-mail:loujunbin1224@163.com

<sup>3</sup> Corresponding author: Maritime School, Zhejiang Ocean University, China, e-mail: ypgong@zjou.edu.cn

degradation, which enjoys broad application prospects in the fields of electronic products, daily chemical products, fresh packaging and fiber tableware [1-4].

However, the current production of pulp molding products face problems such as low automation, low work efficiency, intensive labor, and low raw material utilization, which severely restricts development of the industry. Since the end of 2012, "Machine Substitution" receives gradual popularity in the traditional pulp molding manufacturing enterprises in the Yangtze River Delta and the Pearl River Delta in China. By upgrading traditional industries with modern and automated equipment, it promotes replacement of demographic dividends by technological dividends, and contributes to the optimization and upgrading of traditional manufacturing industries [5-6]. The "machine substitution" mode in the pulp molding manufacturing production process is to comprehensively develop and update traditional loading, unloading and handling, manual paper mold forming and shaping equipment into intelligent equipment with manipulators to replace manual operations, so that the whole process of slip casting, molding raw material transfer, hot pressing and shaping, shaped product loading and unloading and trimming is automatic without manual operations [7].

The rationality of the structure design of the robot end-effector will have a direct impact on the quality stability and efficiency of the product molding process. At present, manipulators are developing towards high speed, high precision and light weight, and its performance is mainly limited by its vibration characteristics [8]. Li *et al.* used rigid-flexible coupling dynamics analysis method to model and analyze the movement characteristics of the loading truss manipulator, and studied the impact of flexibility of key components on the movement accuracy of the truss manipulator [9]. Wang *et al.* used ADAMS to establish a rigid-flexible coupling model to describe and analyze the dynamic characteristics of spot-welding robots during the entire operation process [10].

However, the analysis of dynamic characteristics in the field of industrial robots today mostly focuses on the static and dynamic characteristics of its overall structure [11-14], and there is less analysis on the structural dynamic characteristics of the end-effector of molding robot. Moreover, the end-effector demands light weight optimization design to achieve rapid response during the molding process and improve the stability of the end material transfer process. Topology optimization method based on Finite Element Method (FEM) can provide a lightweight structural model that meets the strength and deformation requirements, which has been effectively implemented in many structural optimization design applications [15-17].

Therefore, this paper takes the key equipment in the pulp molding and shaping process-the end-effector of the transport industrial robot as the research object, and establishes the structure model of the end-effector according to the molding process. Using the ADAMS multi-body dynamics software, the rigid-

flexible coupling dynamic model of the end-effector is built and the motion characteristics are analyzed. The topology optimization method is used to design the lightweight structure of the end-effector, and the optimization performance is verified by ANSYS Parametric Design Language (APDL) and Workbench platform, as shown in Figure 1.

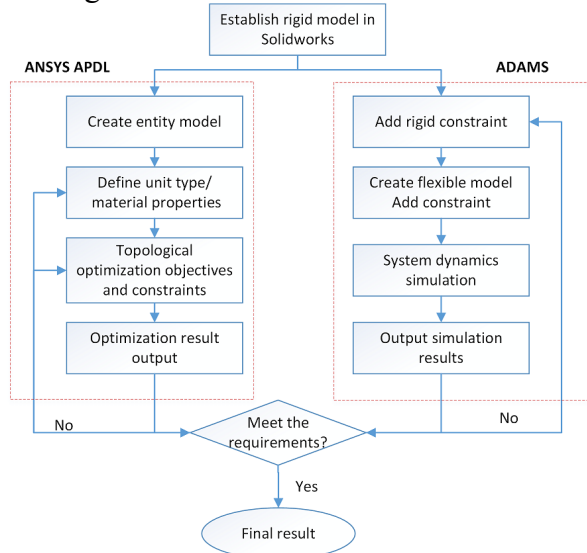


Fig.1. Technical flow chart

## 2. Motion state analysis

### 2.1 Process analysis

The end-effector of this robot needs to perform multiple processes in the production process, specifically as follows:

Process I: The robot takes the material from the molding machine (taking the wet raw material);

Process II: The feeding and taking action of the robot: put the wet raw material on the hot press for processing, and then take the hot pressed dry raw material;

Process III: Unloading action of the robot.

Through the study of the process, it can be known that the robot end structure mainly has the following movement modes, as shown in Figure 2:

- (1) End-effector and profiling mold rotate around the ROTATING PART A;
- (2) End-effector and profiling mold rotate around the BASE A;
- (3) End-effector and profiling mold move back and forth horizontally;
- (4) End-effector and profiling mold move up and down vertically;
- (5) End-effector and profiling mold move obliquely.

In order to make dynamic analysis of the movement of the robot end-effector in the above processes, the dynamic characteristics of the robot in the Process I and Process II will be specifically analyzed, due to these processes basically cover the above-mentioned five kinds of movement modes.

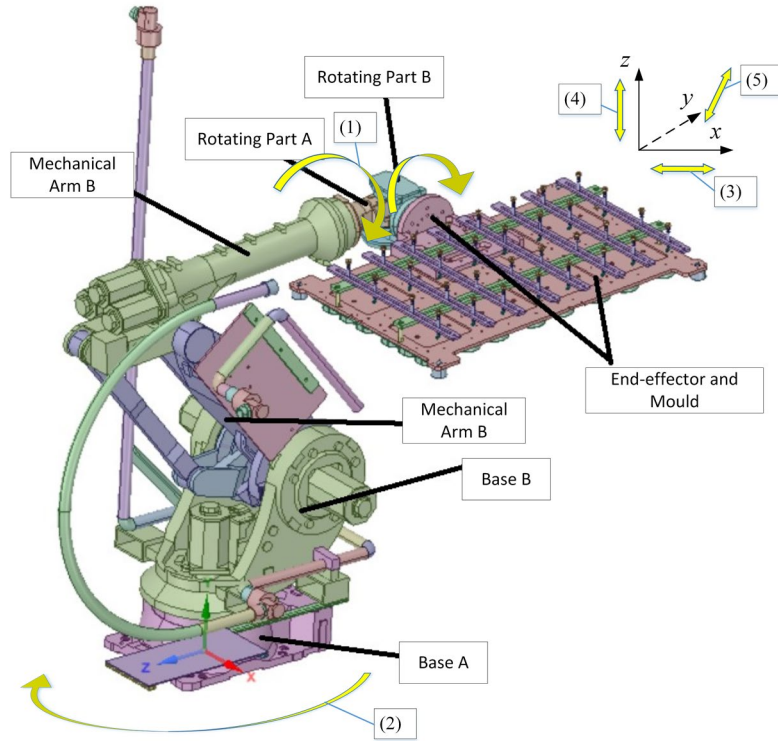


Fig. 2. Movement mode of the robot end structure

## 2.2 Robot structure model

Solidworks is used to establish a three dimensional (3D) model of the robot. To simplify the model, Boolean operation is performed on parts that do not participate in the transmission movement. The bolt connection pre-stress is temporarily not set, and welding process, model size tolerances and assembly errors are not considered. Structural features or components with less performance impact are ignored. The spatial position of the robot end-effector corresponding to the first and second processes are shown in Fig. 3.

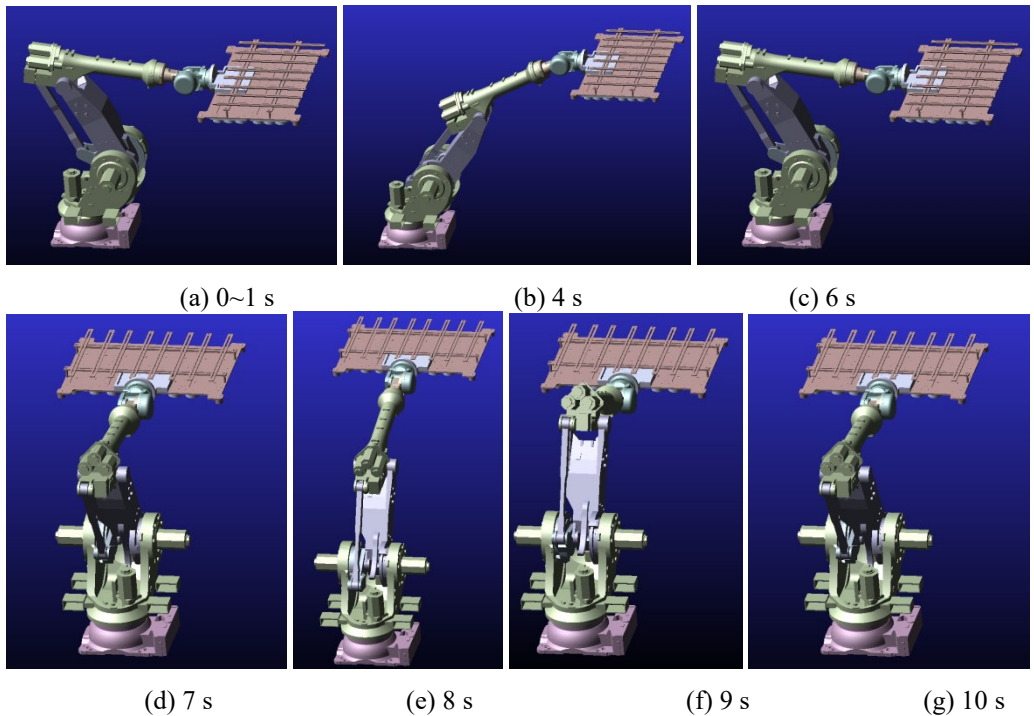


Fig. 3. Spatial position of the robot end structure

### 3. Rigid-flexible coupling analysis of end-effector

#### 3.1 Rigid-flexible coupling model

##### 3.1.1 Coupling model setting

Since the molding robot end-effector is affected by gravity, torque, acceleration factors during its movement, its equivalent stress value will dynamically change. If the rigid body model is used directly, the resulting relevant force, torque, and acceleration values will have deviations. Therefore, for the sake of better simulation accuracy, the robot end-effector is regarded as a flexible body rather than a rigid body, and multi-body dynamics simulation is performed to establish the basis for the subsequent stress analysis of the end structure.

The rigid-flexible joint dynamic model of the robot end-effector is constructed by ADAMS and ANSYS [18-19], and replace the rigid body model of the end-effector with the flexible body file from finite element analysis in ADAMS to build a rigid-flexible dynamic model of molding robot end-effector. Figure 4 shows the flexible body part of the end structure.

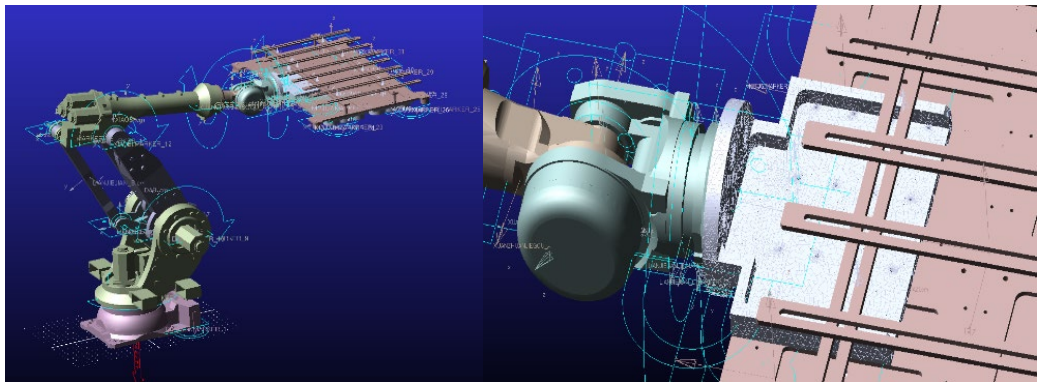


Fig. 4. Flexible end structure

### 3.1.2 Initial state analysis

The initial state analysis of the end-effector model is mainly to determine the spatial position, material settings, load settings, constraint settings, and solver settings.

The material of each part of the robot body is cast iron, and the end structure is aluminum. For the sake of model simplification, the structural features or components with less performance impact are ignored. According to the actual movement posture of the industrial robot, set the revolving pair, the sliding pair between the relative moving parts, and the fixed pair constraints of the robot base and the pin shaft.

In the initial state, the end-effector is affected by the gravity of itself and the profiling mold. At 0.035s, the equivalent stress at the installation connection between the end-effector and the profiling mold (i.e. node 150971) reaches a maximum of 129.84MPa, and the equivalent stress at the fillet connection of the end-effector structure (i.e. node 14978) is 32.2MPa. The initial vibration state of the flexible body stabilizes after about 0.2 s, as shown in Figure 5.

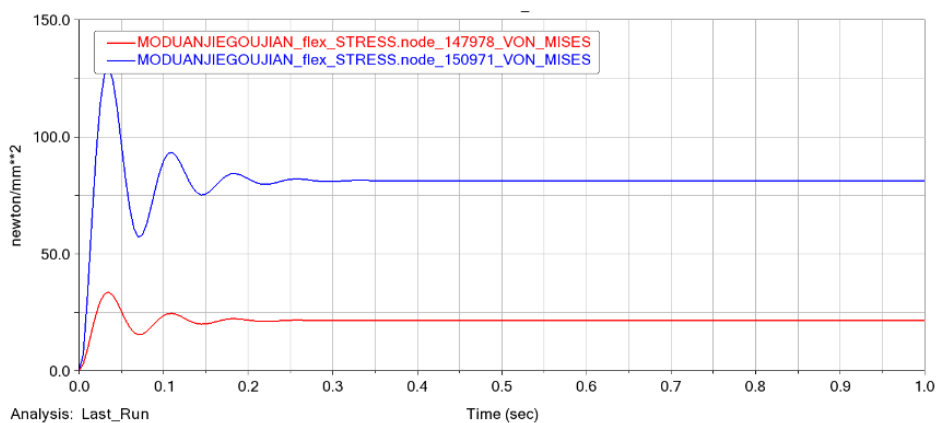
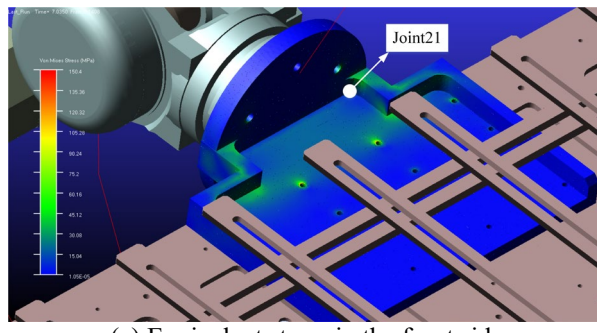


Fig. 5. The equivalent stress changes of the flexible joint of the end structure

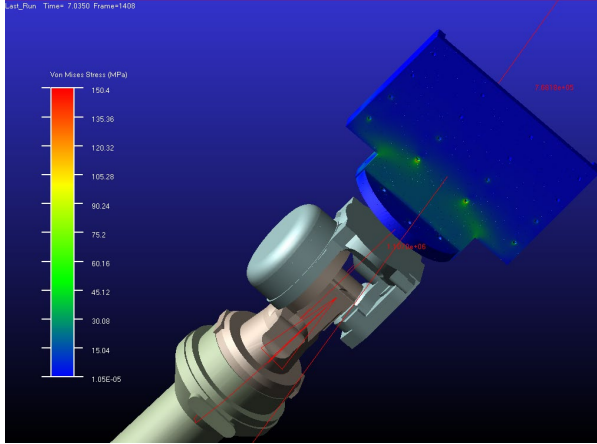
### 3.2 Rigid-flexible coupling analysis results

Taking the initial state analysis results in section 3.1 as the condition of rigid-flexible coupling simulation analysis, the motion states of the end-effector of the robot in the Process I and Process II are simulated and analyzed.

During the movement, the end structure is affected by the force, moment, linear acceleration, angular velocity and angular acceleration factors, leading to dynamic changes in its equivalent stress value. The equivalent stress at the installation connection between the end-effector and the profiling mold (node 150971) reaches a maximum of 150.40 MPa at 7.035 s, and the maximum equivalent stress at the fillet connection of the end-effector structure (node 14978) is 45.3 MPa, as shown in Figure 6. Therefore, the equivalent stress in the working process of the robot end-effector is lower than the yield strength 220 MPa of aluminum alloy material. That is, the structure design strength meets the application requirements.



(a) Equivalent stress in the front side



(b) Equivalent stress in the back side

Fig. 6. Equivalent stress nephogram of the flexible body

In the working process of the flexible end-effector, the movement characteristic change curve of the structure displacement, velocity, acceleration, angular velocity and angular acceleration are shown in the Figure 7.

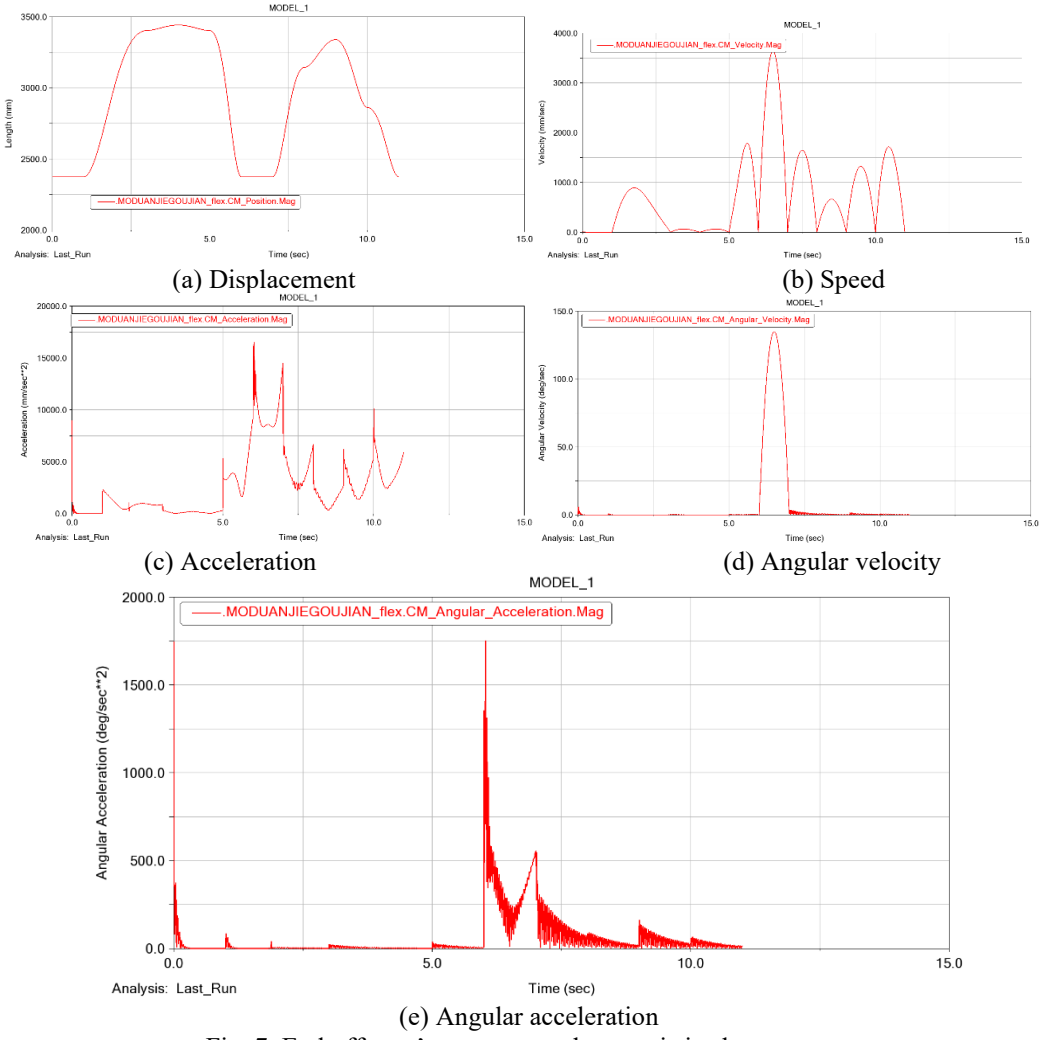


Fig. 7. End-effector's movement characteristic change curve

Fig. 7 shows that in the 11s simulation time, the end-effector completes the two processes of taking and discharging. The effector speed and acceleration fluctuate with the rotation of each joint. When the taking process in the Process I is completed, the speed, acceleration, angular velocity and angular acceleration of the actuator all reach the peak point. At this moment, the effector is in the transition between taking process and discharging process. Due to the flexible body characteristics of the end-effector, its movement characteristic curve will vibrate.

Fig. 8 shows the stress change of the key connection point (Joint21, see in Fig. 6) of the flexible end-effector. Specifically, the change in force load and torque load of the flexible end-effector tends to be consistent with the change in

its acceleration and angular acceleration. At 5.91 s, the effector stress reaches the maximum, the maximum load of key nodes is 3200 N, and the maximum torque is  $2.07 \times 10^6$  N·mm. There is obvious vibration on the load simulation curve of the end-effector, which is in line with the actual working conditions.

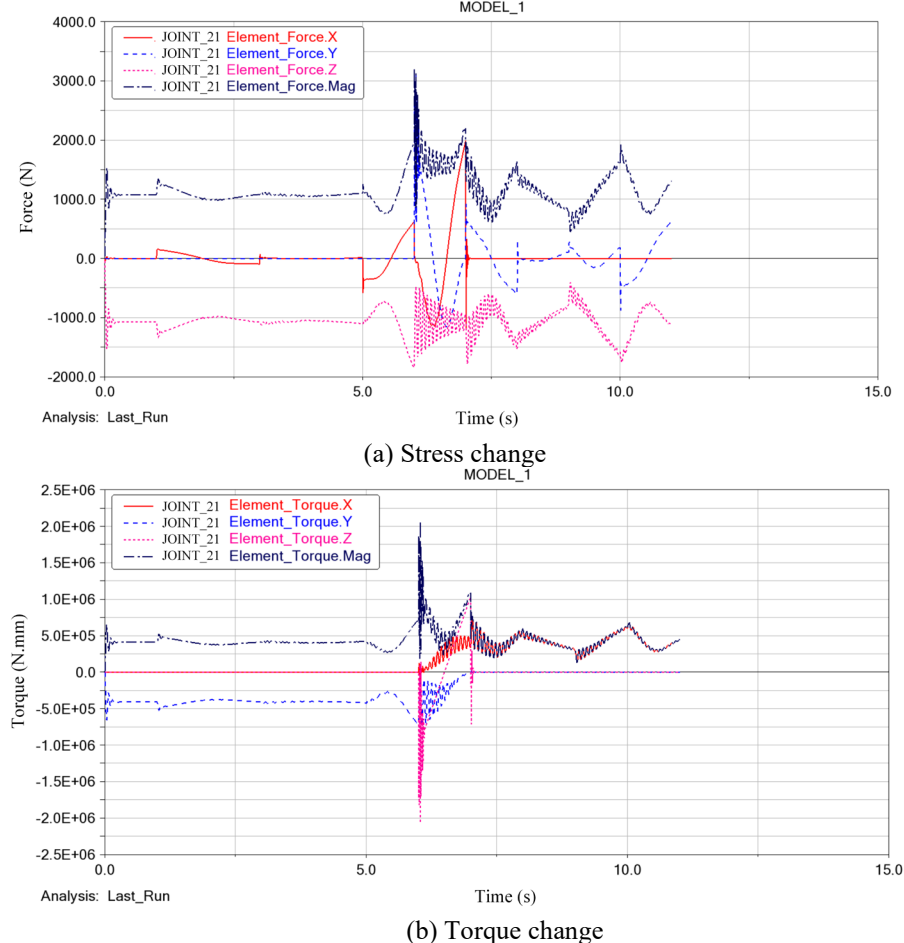


Fig.8. End-effector connection point (Joint21)

#### 4. Optimization design of end-effector

##### 4.1 Topological optimization

Based on the above-mentioned mechanical analysis of the rigid-flexible coupling of the robot end structure, the end-effector is topologically optimized, so that it can meet the performance requirement while reducing the weight for the sake of light weight. At the same time, considering that the static stress and static strain of the end-effector model should not be greater than the yield stress and yield strain of the aluminum alloy material, the optimized mathematical model is:

$$\min F(\rho) = \frac{M(\rho) - M_{min}}{M_{max} - M_{min}} \quad (1)$$

$$\text{s. t. } \begin{cases} \sigma(\rho) \leq \sigma_{max} \\ \sigma(\rho) \leq \sigma_s \\ D(\rho) \leq D_{max} \\ \varepsilon(\rho) \leq \varepsilon_s \end{cases} \quad (2)$$

Where:  $M(\rho)$ ,  $M_{min}$  and  $M_{max}$  are the weight optimization design variables.  $\sigma(\rho)$ ,  $\varepsilon(\rho)$  and  $D(\rho)$  are the stress, strain and the deformation of the end-effector in the static state respectively;  $\sigma_{max}$  and  $D_{max}$  are the maximum stress and maximum deformation of the prototype structure, respectively,  $\sigma_s$  and  $\varepsilon_s$  are the yield stress and the corresponding maximum strain of the end-effector material, respectively. The end structure is optimized, and the final topology result is shown in the Figure 9. On the basis of topology optimization, the end structure needs to be redesigned so that the shape and structure meet the performance requirement with material removed as much as possible, and also the structure has certain usability and observability at the same time, as shown in Figure 9.

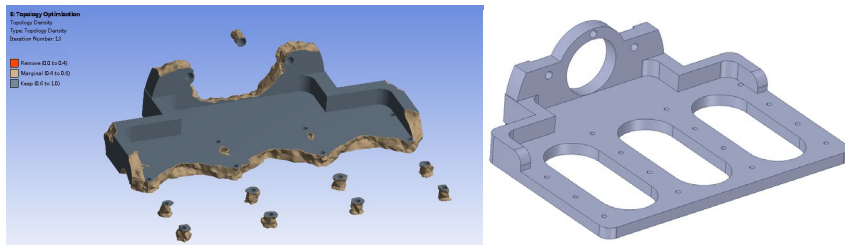


Fig. 9. End-effector structure after topology optimization

#### 4.2 Verification of optimization model

To verify the performance of the topologically optimized end-effector, the same boundary conditions and loads as the structural simulation before optimization were applied through ANSYS APDL and Workbench, and a confirmatory simulation was carried out. The simulation result is shown in Figure 10. The mass of the end-effector structure drops from 16.43 kg to 9.50 kg, a drop of 42.16%. The maximum deformation displacement increases from the original 1.16 mm to 1.29 mm, an increase of 11.2%; the maximum equivalent stress increases from the original 150.40 MPa to 180.21 MPa, an increase of 19.82%.

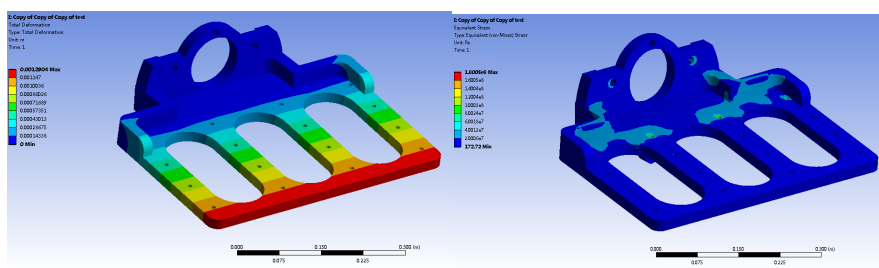


Fig. 10. Structural deformation and equivalent stress after topology optimization

Fig. 11 shows the force change of the key connection point (Joint21) of the flexible end-effector after the topology optimization. Fig. 11 demonstrates that the change trend of the force load and the torque load of the optimized end-effector is basically the same as that before the optimization. At 5.62 s, the effector force reaches the maximum, the maximum force load of the key nodes increases from 3200 N before optimization to 3500 N, and the maximum torque increases from  $2.07 \times 10^6$  N·mm before optimization to  $2.61 \times 10^6$  N·mm. In general, the end-effector achieves lightweight optimization design objective despite the optimization constraints, which guarantees that the mechanical properties of the device meet the optimization goals.

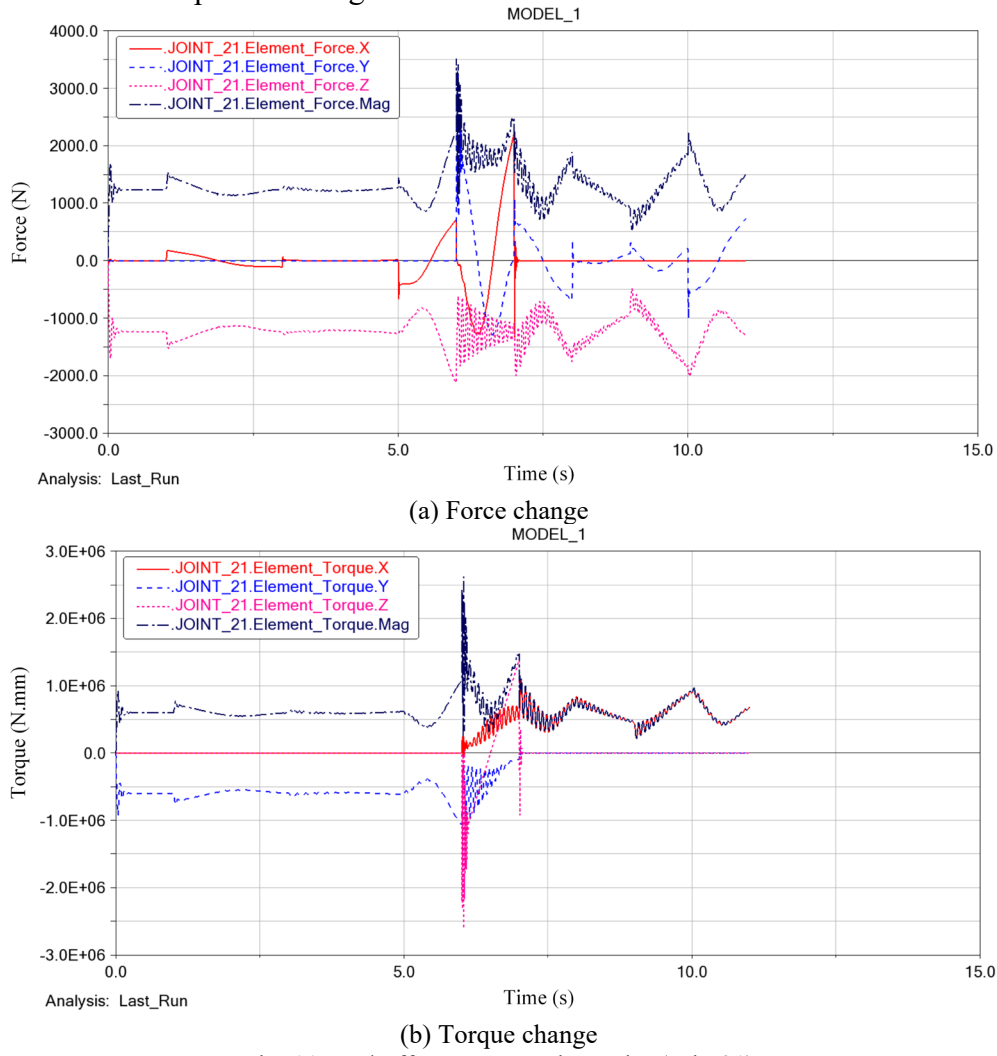


Fig. 11. End-effector connection point (Joint21)

## 5. Conclusions

Taking the end-effector of the pulp molding, forming and shaping transport industrial robot as the research object, according to the molding process, the structure model of the end-effector is established. The rigid-flexible coupling dynamics model of the end-effector is built by using ADAMS, and the movement characteristics are analyzed and topologically optimized. The specific results are as follows:

(1) The equivalent stress value of the flexible end-effector will dynamically change with the change of the force, moment, linear acceleration, angular velocity and the angular acceleration. The equivalent stress at the installation connection between the end-effector and the profiling mold reaches a maximum of 150.40 MPa at 7.035s, and the maximum equivalent stress at the fillet connection of the end-effector structure is 45.3 MPa, both lower than the yield strength 220 MPa of aluminum alloy materials, thus meeting the processing and application requirements of molding pulp products.

(2) The change in force load and torque load of the flexible end-effector tends to be consistent with the change in its acceleration and angular acceleration. At the transition between the two processes, the maximum force load on the key effector nodes is 3500 N, and the maximum torque is  $2.61 \times 10^6$  N·mm. There is obvious load dynamic vibration of the end-effector.

(3) The end-effector has a lightweight structure after the topological optimization design, the mechanical properties of the device are guaranteed while meeting the optimization goal. The mass of the end-effector structure drops by 42.16%. The maximum deformation displacement increases from the original 1.16 mm to 1.29 mm, an increase of 11.2%; the maximum equivalent stress increases from the original 150.40 MPa to 180.21 MPa, an increase of 19.82%.

In the future, it is necessary to further refine and deepen the rigid-flexible coupling modeling analysis on this basis, especially how to accurately establish the rigid-flexible coupling model for industrial robots under actual complex working conditions is a big challenge. Furthermore, for the structural topological optimization design, we need to consider the multi-objective optimization problem in the future.

## Acknowledgements

This work was supported by the science and technology project entrusted by the enterprise (grant number 00520104).

## R E F E R E N C E S

- [1] *Q.Y. Liu, C. Loxton, A.A. Mohamed, M. Jawaid, R. Braganca, R. Elias*, “Development of Pulp Moulded Packaging Samples from Empty Fruit Bunch Fibre”, *Pertanika Journal of Science and Technology*, **vol. 29**, no. 4, 2021, pp. 2901-2912
- [2] *F.D. Zhang, L.J. Wang, X.Y. An, H.B. Liu, S.X. Nie, H.B. Cao, Q.L. Xu, B. Lu*, “Improving Sizing Performance of Middle Layer of Liquid Packaging Board Containing High-yield Pulp”, *Cellulose*, **vol. 27**, no. 8, 2020, pp. 4707-4719.
- [3] *T. Hamouda, A.H. Hassanin, N. Saba, M. Demirelli, A. Kilic, Z. Candan, M. Jawaid*, “Evaluation of Mechanical and Physical Properties of Hybrid Composites from Food Packaging and Textiles Wastes”, *Journal of Polymers & the Environment*, **vol. 27**, no. 3, 2019, pp. 489-497.
- [4] *S.F. Curling, N. Laflin, G.M. Davies, G.A. Ormondroyd, R.M. Elias*, “Feasibility of Using Straw in a Strong, Thin, Pulp Moulded Packaging Material”, **vol. 97**, no. 1, 2017, pp. 395-400.
- [5] *M. Faber*, “Robots and Reshoring: Evidence from Mexican Labor Markets”, *Journal of International Economics*, **vol. 127**, no. 1, 2020, pp. 103384
- [6] *M. E. Virgillito*, “Rise of the Robots: Technology and the Threat of a Jobless Future”, *Basic Books a Member of the Pereus Books Group*, 2015, pp. 1-3.
- [7] *D. Mattia, S. Prateek, B.M. Ellen*, “Moulded Pulp Manufacturing: Overview and Prospects for the Process Technology”, *Packaging Technology and Science*, **vol. 30**, no. 6, 2017, pp. 231-249.
- [8] *M. G. Alkalla, M. A. Fanni*, “Integrated Structure/control Design of High-speed Flexible Robot Arms Using Topology Optimization”, *Mechanics Based Design of Structures and Machines*, **vol. 1**, 2019, pp. 1-22.
- [9] *J.H. Li, P. Ma, J. Liu, N. Liao, H. Zhao*, “Research on Rigid-flexible Coupling Motion Characteristics of Loading Truss Manipulator”, *Machine Tool & Hydraulics*, **vol. 47**, no. 23, 2019, pp. 1-6.
- [10] *X.R. Wang, W. Song, T. Xue, H. Tian*. “Dynamics Analyses of Rigid-Flexible Coupling of Spot-Welding Robot”, *Journal of Advanced Manufacturing Systems*, **vol. 19**, no. 4, 2020, pp. 855-867.
- [11] *S. Kaitwanidvilai, S. Buthgate, H. Aoyama, P. Konghuayrob*, “Robot Arm Structure Design Using Polyamide Evaluated by Finite Element Analysis”, *Sensors and Materials*, **vol. 32**, no. 2, 2020, pp. 487-497.
- [12] *C.C. Ma, D. Jing, M.Y. Shao, H. Yu, Z.H. Guo*, “Dynamical Analysis and Control of Rotatory Manipulators with Time Varying Mass Loads”, *International Journal of Applied Electromagnetics and Mechanics*, **vol. 64**, no. 4, 2020, pp. 307-314.
- [13] *H.T. Luo, J. Fu, P. Wang, J.G. Liu, W.J. Zhou*, “Design Optimization of the Ram Structure of Friction Stir Welding Robot”, *Mechanics of Advanced Materials and Structures*, **vol. 27**, no. 2, 2020, pp. 108-118.
- [14] *P.K. Singh, K.C. Murali*, “Dynamic characteristics of continuum robot for colonoscopy using finite element simulation”, *Proceedings of the Institution of Mechanical Engineers Part C-Journal of Mechanical Engineering Science*, **vol. 235**, no. 22, 2021, pp. 6398-6414.
- [15] *C.L. Chang, C.S. Chen, C.H. Huang, M.L. Hsu*, “Finite Element Analysis of the Dental Implant Using a Topology Optimization Method”, *Medical Engineering & Physics*, **vol. 34**, no. 7, 2012, pp. 999-1008.

- [16] *Y.C. Shi, H.D. Yan, P. Gong, T. Liu, Q.L. Wang, L.C. Cheng, J. Deng, Z.Y. Liu*, “Topology Optimization Design Method for Supporting Structures of Optical Reflective Mirrors Based on Zernike Coefficient Optimization Model”, *Acta Photonica Sinica*, **vol. 49**, no. 6, 2020, pp. 0622001
- [17] *L.S Sha, A.D.Lin, X.Q. Zhao, S. L. Kuang*, “A Topology Optimization Method of Robot Lightweight Design Based on the Finite Element Model of Assembly and Its Applications”, *Science Progress*, **vol. 103**, no. 3, 2020, pp. 0036850420936482.
- [18] *S.Y. Zhang, K. Zhang, B. Song, W.D. Yu, D. Li*, “Dynamic Modeling and CAE Cosimulation Method for Heavy-Duty Concrete Spreader”, *Advances in Civil Engineering*, **vol. 2021**, 2021, pp. 5548678.
- [19] *M.L. Wang, B.G. Wen, Q.K. Han, Y.B. Sun, C.X. Yu*, “Dynamic Characteristics of a Misaligned Rigid Rotor System with Flexible Supports”, *Shock and Vibration*, **vol. 2021**, 2021, pp. 1-16.